

More Contacts MOE-Care: Soft Robotic Perception and Manipulation for Contact-Rich Assistive Care

Author Names Omitted for Anonymous Review.

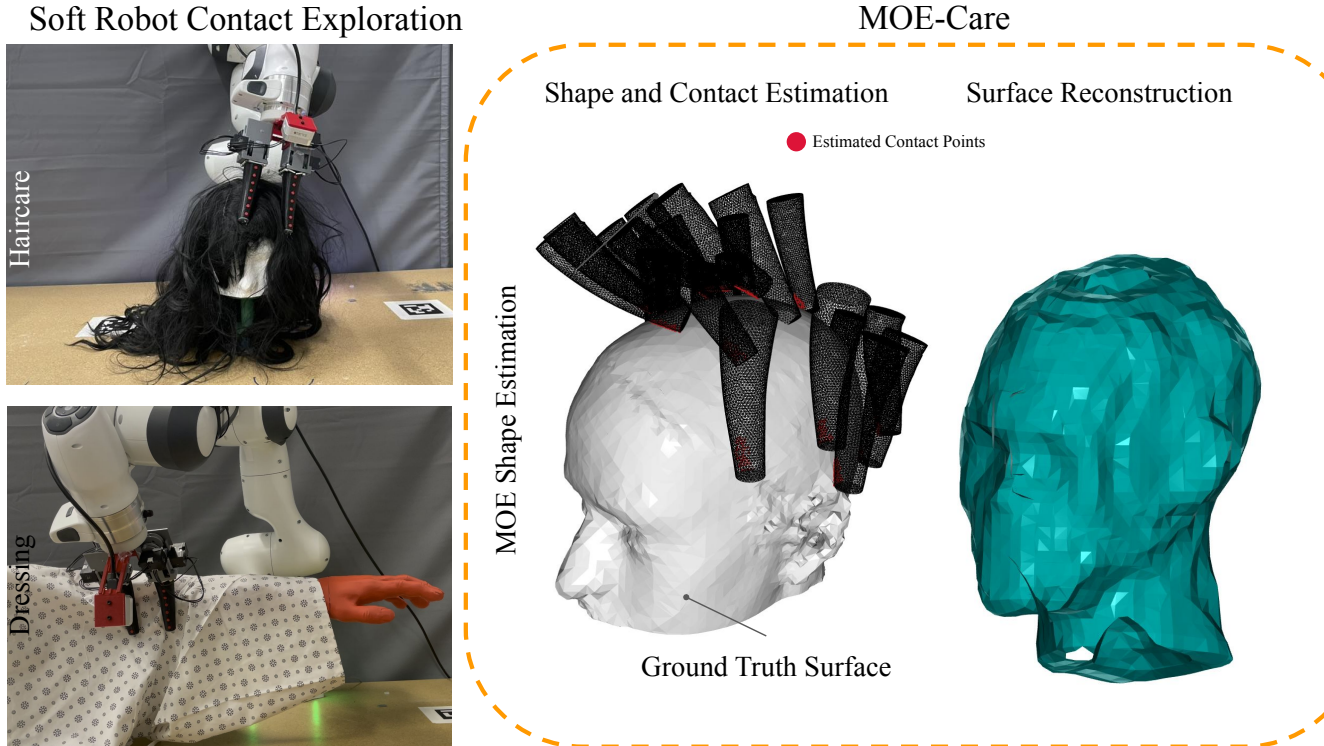


Fig. 1: Toward developing an assistive robot capable of safely interacting with humans even with heavy occlusion, we introduce and demonstrate MOE-Care, an assistive care system to observe soft robotic end-effector deformations, reason about contact conditions with the environment, and reconstruct the geometry of the contacting surface. We first present Multi-finger Omnidirectional End-effector (MOE), a dexterous soft manipulator that is capable of safely interacting with delicate surfaces (left). We use wrist-mounted RGB-D camera observations and mesh optimization-based methods to estimate deformations in MOE. Based on deformed MOE shapes, we estimate contact conditions and reconstruct the occluded surface (right).

Abstract—Many people worldwide require assistance to perform Activities of Daily Living (ADLs). Assistive robots could immensely benefit those with limited mobility by helping with ADLs. Many ADLs require the robotic agent to be able to reason about contact and estimate contacting surface geometries occluded by hair or garment. In this paper, we present MOE-Care, a system for contact-rich assistive care that models contact surfaces under occlusion during interaction. We introduce and test the idea that contact conditions and contact object geometry can be inferred by observing contact deformations in a compliant and soft robot manipulator. Our proposed Multi-finger Omnidirectional End-effector (MOE) is a dexterous soft manipulator that is capable of safely interacting with delicate surfaces. We use a mesh energy optimization-based method to estimate the shape of MOE in interaction with occluded assistive dressing environments such that with MOE-Care, we can accurately register occluded surface contact with an average distance error of 6.25 mm, beating the baseline by 17.53%. We then demonstrate that the MOE shape estimation and contact localization modules can be deployed to reconstruct an occluded surface with averaged errors of 3.62 mm.

I. INTRODUCTION

Approximately 1.3 billion people worldwide experience significant disability [52], which can affect their ability to perform activities of daily living (ADLs) [82]. Robots assisting with ADL tasks have the potential to help reduce health inequality and prolong independence. Many of these tasks require body contact and shape estimation through occlusions caused by hair and garments. This paper proposes hardware design and methods for an actuated soft end-effector for ADLs, and using its compliance for safety, contact estimation, and surface reconstruction under occlusion.

Prior work on assistive robots has studied how robots can provide assistive care for ADLs such as feeding [53, 6, 5, 54, 67], bathing [39, 91, 22, 24, 48], bedding [37, 58, 59], grooming [13, 29, 18, 31], and dressing [33, 21, 36, 43, 44, 90, 77, 66]. Such ADLs often require an assistive robot to

sense, model, and reason about contacts to ensure safe human-robot interaction. Given safety concerns, most prior work rely on using costly or specialized sensors to avoid applying unsafe contact forces to the human body over predetermined thresholds, and explicitly avoiding direct contacts during human-robot interaction. Such constraints can produce overly conservative robot assistance that may be too slow, opaque, and uncomfortable for human users [64, 10, 11, 12, 23].

Instead, we target contact-rich assistive care scenarios for robots to embrace contacts safely rather than avoiding them, to provide better assistance. To this end, soft robot manipulators offer unique advantages compared to rigid end effectors. The inherent compliance of soft robot manipulators [30] enables robust control and mechanically aids in safe real-world operation [40, 4, 49]. This is especially relevant for delicate manipulation [62] and human-robot interaction [56, 25]. People also tend to perceive soft robots as safer and more encouraging to physically touch when compared to their rigid counterparts [35]. Additionally, prior work showed soft robots deform significantly with contact [61, 87], hinting at the possibility of using observed deformations as a signal for contact conditions.

To demonstrate the capability of soft robot manipulators for assistive care, we consider robot-assisted dressing and haircare ADLs, which require the robot to reason about contact with the human body (e.g., limbs or head) under occlusion caused by garments or hair. When humans perform these ADLs themselves, embodiment and haptics provide intuition and feedback of occluded contact surfaces. Correspondingly, for robot-assisted haircare, the robot must reason about the human's head shape under occlusion of varying lengths of hair. This poses a complex problem of distinguishing between the hair, which can be styled, and the underlying skeleton structure of the head. Similarly, with robot-assisted dressing, the human's limbs may be occluded by already worn garments.

In this paper, we present MOE-Care, a system for contact-rich assistive care that perceives deformations of a dexterous soft robot manipulator to model contact surfaces during interaction, by reconstructing 3D surface geometry. MOE-Care tracks the movement of unoccluded keypoints on a soft robot manipulator and reconstructs watertight surface meshes of the deforming soft robot manipulator using a mesh energy-minimization method based on As-Rigid-As-Possible (ARAP) principles [65]. We show that this keypoint mesh optimization-based shape estimation method produces robust, high-fidelity shape reconstructions, providing more 3D shape structure compared to end-to-end learning-based approaches [86]. MOE-Care then uses the observed deformations of the soft robot manipulator to predict points over the mesh that are in contact with other object surfaces. To overcome surface occlusions during assistive care interactions such as robot-assisted dressing and haircare, we update a modified formulation of a Gaussian Process Implicit Surface (GPIS) [83, 20] model with the predicted contact conditions. With MOE-Care, we introduce the idea of reasoning about contact conditions and contacting object geometry from observed deformations

of a soft robotic manipulator, which is an advantage of soft robots. To test MOE-Care in assistive robotics scenarios, we experiment with MOE-Care in haircare and dressing scenarios in simulation and on 3D-printed models. In summary, we make the following contributions:

- the design of MOE, a dexterous two-finger soft robot manipulator for contact-rich assistive care tasks,
- demonstrations of how contact conditions can be inferred by perceiving deformations in MOE as it interacts with other object surfaces.
- MOE-Care, a system that tracks keypoints to reconstruct MOE's deforming 3D surface geometry, localizes distributed contact conditions using the observed deformations, and updates an implicit surface model with the predicted contact conditions over an interaction trajectory to reconstruct the occluded contacting surface, and
- experiments testing the capability of MOE-Care to reason about contact for real-world contact-rich robot-assisted dressing and haircare ADLs.

II. RELATED WORK

A. Assistive Robotics

Extensive prior work has explored assistive robots to support ADLs such as feeding [53, 6, 5, 54, 67], bathing [39, 91, 22, 24, 48], bedding [37, 58, 59], grooming [13, 29, 18, 31], and dressing [33, 21, 36, 43, 44, 90, 77, 66]. Several surveys [7, 81, 50] provide a broad overview.

Counter-intuitively to the purpose of assistive robotics, much of the prior work avoids direct human-robot contact to ensure human safety. For instance, Li et al. [43] develop a motion planner for robot-assisted dressing that frames human safety in terms of collision avoidance or safe impacts when collisions are unavoidable. Wang et al. [77] transfers point cloud-based assistive dressing policies, trained by reinforcement learning in simulation, to the real world. Their reward function includes a penalty term for when the robot end-effector moves too close to the limb. By using rigid robot end-effectors and avoiding contacts, these works can dress only loose garments onto human arms. Hughes et al. [31] detangles hair from various wigs types using a hair brush that is attached to a load cell and mounted on a robot arm's end-effector, with the distance between hair and brush fixed to some predetermined value. Dennler et al. [18] propose a system for robot hair combing on wigs using RGBD inputs. They produce motion plans over the hair surface using only the outer appearance, without considering the occluded head. In their virtual survey, some participants commented that the rigid robot's use of force looked rough and seemed to lack a sense of touch.

Some studies on contact-rich assistive robotics propose soft wearable assistive robotic devices that specialize in a specific task such as bathing [45], rehabilitation [55, 57], or supporting limbs with limited mobility [51]. In this paper, we introduce a dexterous soft robot manipulator that has only a single wrist-mounted camera, to be more broadly suitable for contact-rich assistive care.

B. Soft Robot Manipulators and Perception

The compliance and deformation of soft robot manipulators [30] pose a challenge for perception and sensing [74] to determine the manipulator’s proprioceptive state. Soft robot proprioceptive sensing and shape representations must capture complex deformation patterns of the soft robot [86, 87].

Conventionally, the shape of soft robots has been represented by parameterized 2-dimensional curves, which effectively reduces the state estimation problem by modeling more tractable, low degrees-of-freedom systems. The most compact state representation uses a single degree-of-freedom curve with constant curvature, defined by its bending radius [16, 85]. More expressive representations construct multiple geometric primitives such as piecewise constant curvature models [17], multiple rigid frames [46], or rigid links [60]. These primitive representations have been used for dynamic control of soft robot manipulators [8, 3, 28]. However, these representations fail to accurately capture volumetric information, and more complex deformation behaviors such as distributed, contact-based deformations [86]. Some methods have been proposed to capture richer soft robot state using point clouds [75, 86], but they rely on learning a state estimation model to reconstruct shapes by training on thousands of calibration samples. Recent work grounds shape reconstruction with mechanics-based priors, which yields more data efficiency and stable proprioceptive state estimation [70, 87]. In this paper, we show how these methods can be extended beyond manipulator-only proprioceptive state estimation to object interaction and robotic manipulation, by reconstructing object contacting surfaces based on deformations of the soft manipulator.

C. Contact-based Surface Reconstruction

We leverage the insight that deformations can provide useful physical signals to infer contact points, maps, or forces [34, 32, 84, 89, 78, 41, 40, 27, 26, 14]. Specialized tactile sensors such as GelSight [89] and Digit [41], when attached to rigid end effectors [67], infer contacts from deformations. Although such sensors can provide high-fidelity tactile and texture information about the contacting surface, they require contacts to occur on the small sensorized contact region, which strongly constraints sensor configuration when used in robot manipulators [69]. Prior work showed soft robot manipulators deform significantly with contact [61, 87]. In this paper, we show how contact deformations of a soft robot manipulator can be utilized to reconstruct 3D contact surfaces under occlusion during interaction.

Tactile sensors have enabled robots to perceive objects during contact interactions, even under significant visual occlusions [68, 69] that lead to pose and shape uncertainty [73, 2]. Suresh et al. [68] use data captured from a GelSight tactile sensor and depth camera to build a Gaussian Process spatial factor graph as an implicit surface representation. Recent methods have also been proposed that do not use tactile sensors, but instead estimate contact surfaces of unactuated deformable objects. Wi et al. [79, 80] use continuous implicit surface representations to reconstruct the shape, contact points,

and contact forces of a deforming spatula mounted as a robot end-effector while pressed against a tabletop surface. Van der Merwe et al. [72] propose an implicit representation that uses visuo-tactile data to estimate the deforming geometry and contacts of a cube sponge mounted as a robot end-effector while pressed against a YCB mug or bowl [9]. These approaches operate directly on point clouds, and assume static interactions between a single tool and the environment. In contrast, we propose reconstructing the deforming geometry of a multi-fingered soft robot manipulator, and we update an implicit surface model with an interaction trajectory.

III. METHOD

In this section, we describe the design of our dexterous soft robot manipulator MOE (Section III-A); proprioceptive sensing for MOE that reconstructs its deforming surface geometry (Section III-B); contact estimation based on observed deformations in MOE (Section III-C); and reconstruction of contacting surfaces using predicted contact conditions over an interaction trajectory (Section III-D).

A. MOE Design

We designed a soft tendon-driven manipulator which we call Multi-finger Omnidirectional End-effector (MOE), inspired by a single-finger tendon-driven soft robot from Yoo et al. [87]. As shown in Fig. 4, MOE has two soft fingers molded from silicone with low hardness (Ecoflex 00-30, Smooth-on). Each finger has four tendons embedded that are actuated by two servo motors (DYNAMIXEL XC330-M288-T, Robotis). Each pair of tendons actuated by a single servo motor controls MOE finger’s range of motion in a bending plane. The design is largely modular, where each of the fingers is an independent subsystem that can be detached. MOE design can be extended to variants with more fingers as needed. In the scope of this work and the task of hair grasping that we looked at, we determined that two fingers were sufficient. We placed an RGB-D camera (Realsense D405, Intel) on the wrist of MOE to provide egocentric-view depth images. Red markers are placed on the surfaces of the MOE fingers for the RGB-D camera to track MOE keypoints as the body deforms.

B. MOE Sensing

Shape estimation and representation for soft robots is a challenging problem because of their complex and high degree-of-freedom deformation behaviors [70, 86, 87]. Previous works have proposed both explicit representations of deformable bodies such as meshes [87] and implicit representations such as neural signed distance functions [72]. Explicit representations are particularly convenient for this work because we can directly leverage the reconstructed body’s nodes and their correspondences for downstream tasks such as contact surface reconstruction.

The goal of the MOE estimation pipeline is to infer the overall mesh of the MOE based on the observation of sparse keypoint movements. We extend a previously proposed POEM pipeline to multiple fingers [87]. The working principle

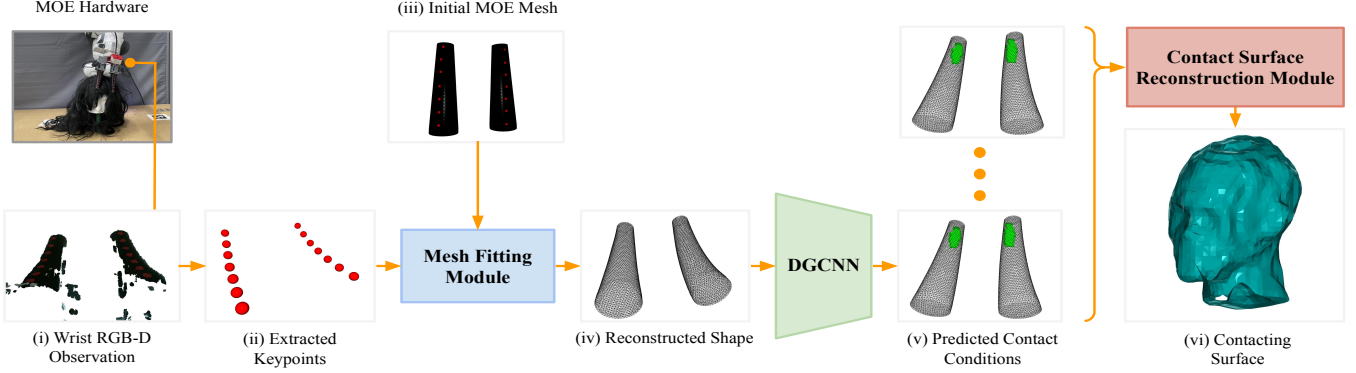


Fig. 3: Overview diagram of the MOE-Care system for interactively understanding geometry for assistive care tasks. (i) We capture RGB-D observations from the wrist camera during interaction. (ii) We extract keypoints on each finger of MOE. (iii) Using the initial MOE mesh and extracted keypoints, we fit a mesh to the deforming state of MOE. (iv) We reconstruct MOE’s deforming surface geometry. (v) We use a DGCNN which was trained in simulation to estimate real-world contact conditions (vi). Using the predicted contact conditions for an interaction trajectory, we reconstruct the contacting surface under occlusions.

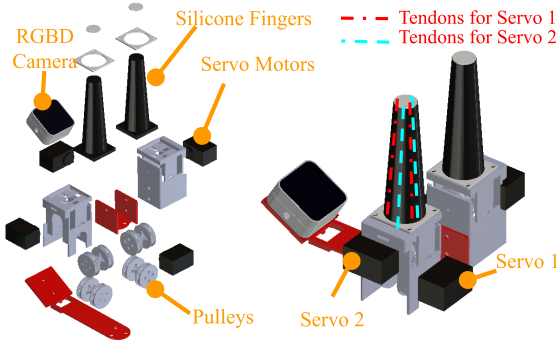


Fig. 4: **MOE end-effector design.** Left: exploded view and assembly of MOE. Right: fully assembled MOE.

of POE-M pipeline relies on As-Rigid-As-Possible (ARAP) which is framed as an energy minimization problem over mesh nodes [65].

To guide the shape estimation of MOE, we track the 7 red keypoint markers placed on each of the surfaces of MOE fingers, as shown in Fig. 5-A. We segment the markers using color thresholds, and apply DBSCAN to cluster the 3D points and find their centers. In the initial frame, we find the nodes on the initial mesh closest to the keypoints and use them as handle points. From the initialization phase, we account for the movement of each of the keypoints frame-to-frame. In practice, some of the keypoints may become occluded due to hair getting in the way. To account for this, we remove the occluded keypoints from consideration in the ARAP mesh fitting phase.

To deform the mesh based on the keypoint movements, we

define the source surface mesh S and the deformed mesh S' . As previously proposed [42, 87], we include a penalty on the rotations of the neighboring edges to produce mesh updates that are physically admissible. The energy to minimize is:

$$E_{\text{smoothed}}(S, S') = \min_{R_1, \dots, R_m} \sum_{k=1}^m \left(\sum_{i,j \in e_k} c_{ijk} \|e_{ij} - R_k e_{ij}\|^2 + \lambda \hat{A} \sum_{e_l \in N(e_k)} w_{kl} \|R_k - R_l\|^2 \right).$$

For reconstructing the full mesh shape of MOE, we treat vertices corresponding to the keypoints $p_{1, \dots, |p_k|}$ as being constrained to the new positions, based on the predicted keypoint positions, while the rest of the mesh vertex positions are moved to minimize E_{smoothed} .

C. Contact Estimation

Contact points are difficult to obtain directly from the real world because of occlusions from the contacting object. Previous works have demonstrated the capabilities of soft-body simulation to generate training datasets of deformed shapes and contact information [63, 86]. We extend on these works to generate a dataset of fully simulated MOE deformations and contact points.

To sample from varying contact normals and surface orientations, we import objects from the YCB Object and Model Set [9] into a SOFA simulation environment [1]. We also generate and import tendon-actuated meshes of MOE. As shown in Fig. 6, we randomize the selected contacting object’s orientation and position with respect to MOE’s trajectory, to simulate various contact locations and orientations. From these simulated trials, we generated a dataset of 31,722 meshes and corresponding contact points, which were recorded as the indices of the MOE mesh nodes that were in contact with an object.

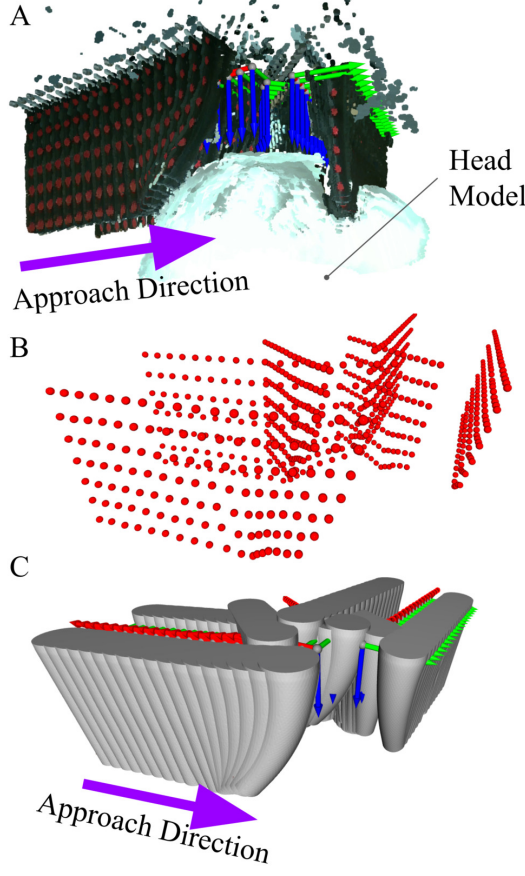


Fig. 5: MOE shape reconstruction from contact with a model head. A: Registered point clouds of MOE touching the head. B: Extracted keypoint positions. C: Reconstructed MOE mesh shapes.

For MOE-Care, we seek to use the shape estimation of the deformed MOE to infer its contact conditions. Highly expressive graph neural network architectures have been demonstrated to be able to learn and reason about complex physical interactions [76, 71]. We train a Dynamic Graph CNN (DGCNN) [76] on the simulated dataset, where the inputs are MOE point clouds generated as described previously. We then use this DGCNN directly on real-world MOE point clouds, to predict the contacting nodes as MOE deforms during an interaction trajectory, as shown in Fig. 5.

D. Contacting Surface Reconstruction

MOE-Care's shape estimation and contact localization modules can provide accurate contact information. However, the number of MOE touches is practically constrained by time and comfort. Hence, the system should sample across the entire surface efficiently as shown in Fig. 1. To effectively generate manipulation actions, we need a robust method to capture the surface uncertainty and integrate sensor measurements in a probabilistic manner. By utilizing the uncertainty measure,

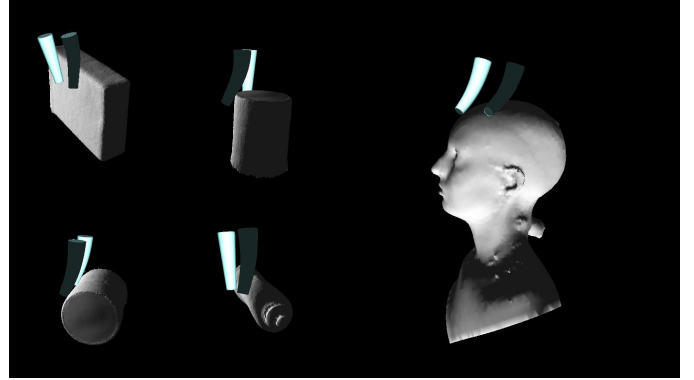


Fig. 6: Simulation environment for generating training data for MOE-Care contact and normal estimation modules. We train the models with YCB objects in random poses.

effective exploration of the surface region can be accomplished using the manipulator. We approach the problem in three incremental steps.

1) *No Prior*: A naive approach for surface reconstruction is a non-probabilistic method by fitting a sphere to the contact points collected in the simulation. Given a set of points $\{\mathbf{P}_i\}_{i=1}^N$, where \mathbf{P}_i is the i^{th} point in 3D space, the objective function for fitting a sphere to the points is defined as:

$$f(\mathbf{c}, r) = \sum_{i=1}^N \left(\sqrt{\sum_{j=1}^3 (P_{ij} - c_j)^2} - r \right)^2$$

where $\mathbf{c} \in \mathcal{R}^3$ represents the center of the sphere, and r is its radius. The initial guess for the optimization is:

$$\mathbf{c}_0 = \frac{1}{N} \sum_{i=1}^N \mathbf{P}_i$$

$$r_0 = \frac{1}{N} \sum_{i=1}^N \sqrt{\sum_{j=1}^3 (P_{ij} - c_0)^2}$$

We solve the optimization problem using L-BFGS to find the \mathbf{c} and r that minimize $f(\mathbf{c}, r)$:

$$\min_{\mathbf{c}, r} f(\mathbf{c}, r)$$

We sampled a point cloud given for the sphere and implemented a k-d tree-based nearest neighbor search to average the residuals between the contact points and the spherical mesh. Finally, we smooth out the abrupt changes to the mesh using a smoothing Laplacian filter.

2) *Spherical Prior*: Gaussian Processes have been extensively studied for implicit surface reconstruction in the literature [83, 20, 68]. We implemented a modified version of GPIS that runs on GPU, to represent the Signed Distance Functions (SDFs) of the heads without needing surface normals. Generally, active exploration algorithms assume an initial condition of uniformly distributed points in a grid. Every measurement

TABLE I: MOE Shape Estimation Evaluation.

| Contact Condition | # of Keypoints | Performance Metrics [mm] | |
|-------------------|----------------|--------------------------|----------|
| | | Avg. CD ↓ | Max CD ↓ |
| Side | 7 | 1.16 | 3.19 |
| Side | 4 | 1.23 | 3.47 |
| Back | 7 | 1.17 | 3.18 |
| Back | 4 | 1.19 | 3.35 |

reduces the uncertainty till the final shape of the object is represented by the GP mean.

We fit a spherical mesh to the points as aforementioned and use this sphere as a prior to train the GP over a dense 3D array of grid points encompassing the mesh. The SDF values for each point P_i are computed as:

$$SDF(P_i) = r - \|P_i - \mathbf{c}\|$$

Given a set of dense grid points \mathbf{X} and corresponding SDF values \mathbf{Y} , the GP model is defined as:

$$f(\mathbf{x}) \sim \mathcal{GP} \left(c, \sigma^2 \exp \left(-\frac{\|\mathbf{x} - \mathbf{x}'\|^2}{2l^2} \right) \right)$$

with the observation model:

$$y = f(\mathbf{x}) + \epsilon, \quad \epsilon \sim \mathcal{N}(0, \sigma_n^2)$$

The training objective is to maximize the marginal log-likelihood loss:

$$\begin{aligned} \log p(\mathbf{Y}|\mathbf{X}) = & -\frac{1}{2} \mathbf{Y}^\top (\mathbf{K} + \sigma_n^2 \mathbf{I})^{-1} \mathbf{Y} - \frac{1}{2} \log |\mathbf{K} \\ & + \sigma_n^2 \mathbf{I}| - \frac{n}{2} \log 2\pi \end{aligned}$$

where \mathbf{K} denotes the covariance matrix constructed using an RBF kernel over the training inputs. Once we have a spherical prior, the GP is updated with the contact point information to obtain the posterior SDF. Finally, the head mesh is reconstructed using Poisson Surface Reconstruction (PSR) [38] on a point cloud obtained by running the Marching Cubes Algorithm (MCA) [47] over the zero-level set of the SDF.

3) *Task-Dependent Prior*: Finally, as the core method of MOE-Care surface reconstruction module, we propose to use a task-dependent prior mesh specific to the domain. For the initial task of reconstructing a human head, we used an open-sourced canonical head 3D mesh and trained a GP to learn a prior over the SDF of the mesh same as before. Once the prior was trained, the GP was fine-tuned on the real-world contact points and the same pipeline of PSR with MCA was used for mesh reconstruction.

IV. EVALUATION

A. Shape Estimation

Prior work has shown that the rigidity and rotation regularization of the ARAP formulation as presented in Section III-B generally produces more physically admissible deformed soft bodies, compared to end-to-end learning-based methods [87]. A key difference in our implementation of the ARAP-based

TABLE II: Contact Estimation Evaluation.

| Method | Object | Performance Metrics [mm] | |
|---------------------------|-------------|--------------------------|--------------|
| | | Avg. CD ↓ | Max CD ↓ |
| MOE-Care [Ours] | Head (Bald) | 6.58 | 13.88 |
| Classification [Baseline] | Head (Bald) | 7.76 | 12.81 |
| MOE-Care [Ours] | Head (Wig) | 12.22 | 21.54 |
| Classification [Baseline] | Head (Wig) | 13.73 | 23.74 |
| MOE-Care [Ours] | Arm (Gown) | 6.24 | 16.56 |
| Classification [Baseline] | Arm (Gown) | 6.88 | 14.45 |

TABLE III: Surface Reconstruction Evaluation.

| Method | Object | Performance Metrics [mm] | |
|----------------------------|-------------|--------------------------|--------------|
| | | Avg. CD ↓ | Max CD ↓ |
| GP w/ Task-Dependent Prior | Head (Bald) | 3.64 | 16.15 |
| | Head (Wig) | 3.62 | 16.36 |
| GP w/ Spherical Prior | Head (Bald) | 13.83 | 35.75 |
| | Head (Wig) | 14.41 | 37.78 |
| Non-Probabilistic Method | Head (Bald) | 16.01 | 36.59 |
| | Head (Wig) | 16.05 | 38.38 |

soft robot reconstruction is that the wrist-mounted RGB-D camera can only observe one side of MOE’s soft surface. The underlying assumption with such an implementation choice is that the observation of one side of MOE can directly inform us about the changes to the state of the other side. As a consequence, we also assume that the cross-section of MOE’s fingers remains largely the same, to allow us to infer the opposing surface’s transformation. This assumption is supported by previous works in mechanics-based modeling and validation of tendon-driven soft robotic manipulators [46].

To validate shape fidelity and consistency on the side of MOE that is normally occluded from the wrist-mounted RGB-D camera, we conducted experiments as shown in Fig. 7. A third-person view high-resolution RGB-D camera (Zivid, One Plus) was placed facing MOE from either its side or the back, to capture the side that is normally unobserved in our pipeline. Then, a clear acrylic sheet was placed facing the third-person view RGB-D camera. This setup allows us to deform MOE against the clear sheet with a large contact surface, while remaining fully observable to the third-person view RGB-D camera. We present the averaged and maximum unidirectional Chamfer Distance (CD) results from third-person RGB-D point cloud to the complete estimated shape, for both side and back contact conditions, in Table I. We can observe that the shape estimation average CD error is small at 1.16-1.17 mm for the two contact conditions. Notably, the error is significantly smaller than the 4.89 mm best average CD error reported in [87]. Such results highlight a potential advantage of directly observing keypoint movements with wrist-mounted cameras compared to indirectly inferring keypoint movements.

We also experimented with testing the robustness of the MOE shape estimation module by removing markers from being considered during ARAP mesh optimization. With 4

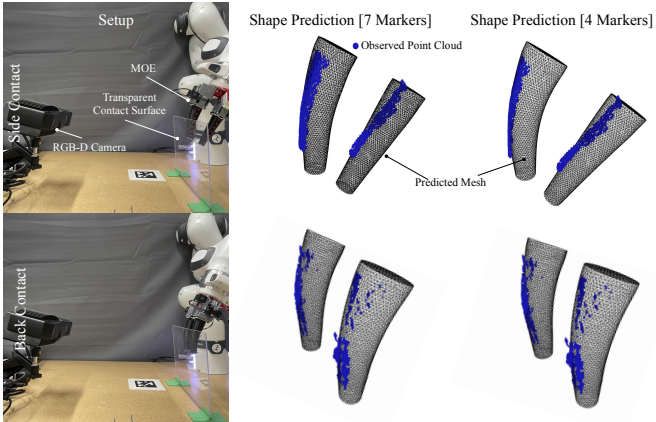


Fig. 7: MOE shape estimation evaluation experiment setup and results. The point cloud is captured from a third-person RGB-D camera and registered to the estimated to the estimated MOE mesh shape. We tested side and back contact conditions against a clear acrylic plate. We also tested cases where all 7 markers on each finger were used for shape estimation and compared to using only 4 of the markers on each finger as summarized in Table I.

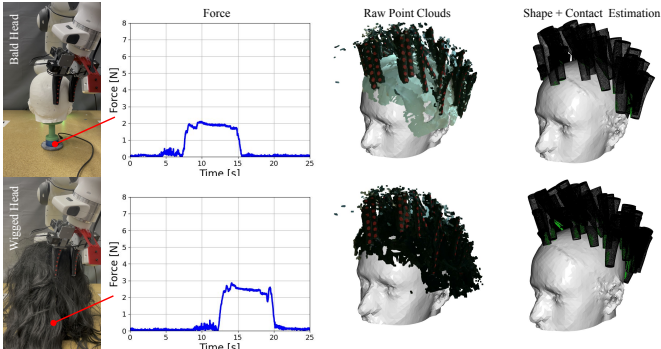


Fig. 8: **Contact estimation experiment results.** The experimental setup for the head contact estimation experiments where a 3D-printed head is mounted on a force-torque sensor. The net force readings are plotted, showing the interaction forces experienced by the head. We also show the registered wrist-mounted RGB-D camera point clouds from the 30 contact conditions. We then also show the predicted MOE shape and contact points on the head. We show these results for the head with and without a wig.

markers, we noted a marginal increase in both average and maximum CD errors from when the shape estimation module considered the full set of 7 markers for each finger. The relatively small change in performance highlights the robustness of the shape estimation module, which can be partially attributed to the well-tuned smoothing penalty to produce meshes that conform well to soft body mechanics.

B. Contact Estimation

To validate MOE-Care’s contact estimation module, we tested the contact estimation module on two different ADL

environments: haircare and dressing. Both environments are motivated by common contact-rich ADL task settings, where visual occlusion may be common and unavoidable, that require the robot to safely interact with the human subject. For the haircare environment, we randomly selected a head mesh of an adult person from a craniofacial shape dataset [15] and 3D-printed it with 1:1 scale. We then mounted the 3D-printed head on a high-resolution force-torque sensor to measure the interaction forces on the head with each MOE contact motion as shown in Fig. 8. From the plot of the net force applied onto the head from MOE for the head with and without a wig, we note that the force remains below 3.0N, even with large deformation contact conditions. Such applied forces are several orders of magnitude lower than the amount of force that can cause blunt trauma [88], suggesting MOE is inherently safe during close-contact interactions.

We then tested 30 distinct MOE contact conditions on the head and evaluated shape and contact estimation modules with and without a wig. We registered the point clouds together from the wrist-mounted RGB-D camera to show the contact coverage across the head in Fig. 8. We then evaluated the shape and contact estimation modules by registering the predicted contact points together and computed unidirectional average and maximum CD from the contact points to the head ground-truth mesh nodes. We then performed a similar series of 15 contact trials on a model of an adult human arm occluded by a hospital gown as shown in Fig. 9. Similar to the trials with the model head, we registered the predicted contact points, compared to the ground-truth mesh, and computed the CD metrics. These results are summarized in Table II.

We can note that in all three ADL environments, the MOE-Care pipeline performs functionally well. The environments with the bald head and arm both resulted in an average CD error of around 6.5 mm. We can notice a noticeably higher CD error of 12.22 mm in the environment with a head and a wig. A significant portion of the error may come from the thickness that the wig’s inner hair net which was measured to be around 5mm thick. Because we do not have a separate ground-truth mesh for the head with a wig, we still evaluated the metrics with the bald head mesh.

As a baseline, we chose to evaluate a method inspired by Zöller et al. [92] which addressed the most similar problem to the one outlined in this work. In the original formulation of the approach the researchers fitted a k-nearest neighbor (KNN) model to classify which discrete region of the finger the robot is making contact with based on acoustic signals [92]. Inspired by this approach, we fitted a KNN to classify whether the contact was happening from the tip, middle, or base of MOE based on the keypoint positions. A KNN model was fitted with a randomly selected subset of the simulation dataset from Section III-C. Then, for evaluation, we use the centroid of the classified MOE finger segment as the single contact point from each contact condition. This is a notably different formulation of Zöller et al. [92] in that we still use MOE-Care’s shape estimation pipeline to map the contact segment classification to a point in the world frame that can be evaluated. We can

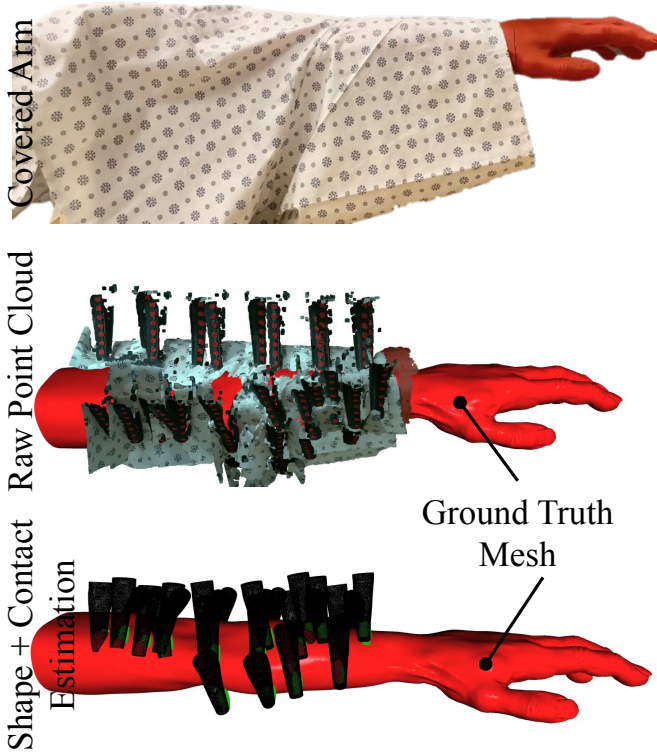


Fig. 9: Experimental setup and results for an assistive dressing environment. Top: setup of a 3D-printed arm covered in a standard hospital gown that is occluding the pose and shape of the arm. Middle: the registered point clouds from the wrist-mounted camera captured at 15 distinct contact conditions. Bottom: estimated shape and contact points of MOE as it interacts with the arm. Note that the ground truth mesh is exposed only for visualization and evaluative purposes and the real-world experiments were only carried out with the hospital gown on the arm.

also note that a significant difference with such approaches is that they produce only a single contact point while MOE-Care produces relatively dense multiple contact points distributed over a small region on the finger. The full comparison results are outlined in Table III-C.

We can observe that on the average CD error metric, the proposed MOE-Care pipeline for MOE shape and contact estimation performed significantly better in all three cases. The biggest difference was observed with the head without a wig where MOE-Care resulted in 17.93% lower average CD error compared to the baseline model. We can also note that KNN model performed relatively consistently and similarly to the proposed MOE-Care pipeline on the maximum CD error metric. In both head without wig and arm environments, KNN model with the MOE-Care shape estimation module had a lower maximum CD error. This is possibly explained by the fact that using the centroid of the predicted region as the contact point generally prevents large outlier predictions. The baseline method also demonstrates the MOE-Care pipeline's

versatility in that the modules within it can be replaced with a different method and can still function well.

C. Contacting Surface Reconstruction

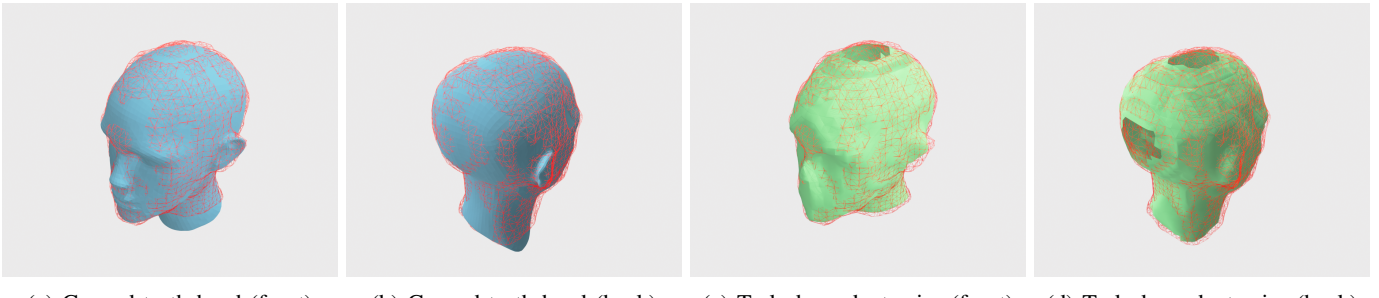
As outlined in Section III-D, we implemented a task-dependent prior as a GP for surface reconstruction from real-world contact points. As shown in Table III, our method reconstructs the mesh from real-world contact points with an average Chamfer distance of 3.64 mm for the bald head, and 3.62 mm for the head with a wig. The capability of the task-dependent prior method to generate a watertight mesh after accommodating real-world data is shown in 10.

We also present a baseline method based on the prior works that assume a primitive geometric shape as initialization for interactive perception and mesh reconstruction [68, 19]. We use a spherical prior as a naive method to obtain the posterior distribution over the real-world contact points. The sphere-prior baseline significantly worse performance with average and max CD values of 13.83 mm and 35.75 mm for bald head data, and 14.41 mm and 37.78 mm for head with a wig respectively. The key point of failure in this method can be attributed to the fitted sphere mesh with points that are significantly out of distribution from an average human head in both positive and negative SDF space.

Finally, to compare GP-based probabilistic methods with a non-probabilistic baseline, the final method uses only the nearest neighbor information for mesh deformation which results in a qualitatively worse formed surface compared to the GP method with a spherical prior. This method performs the worst for surface reconstruction with average and max CD values of 16.01 mm and 36.59 mm for bald head data, and 16.05 mm and 38.38 mm for head with a wig respectively. Our proposed task-dependent prior-based surface reconstruction module performs significantly better than the two baseline methods, resulting in 73.68% and 77.26% reduced average CD metric error for the head without a wig compared to using a spherical prior and the non-probabilistic method, respectively.

V. CONCLUSION

In this work, we introduce a unique system for contact-rich assistive care that models contact surfaces under occlusion during interaction. We developed a dexterous soft manipulator that we call Multi-finger Omnidirectional End-effector (MOE) that is capable of safely interacting with delicate surfaces. We use a mesh energy optimization-based method to estimate the shape of MOE in interaction with occluded surfaces. We demonstrate with haircare and assistive dressing environments that with MOE-Care, we can accurately register occluded surface contact with an average distance error of 6.25 mm, beating the baseline by 17.53%. We then demonstrate that the MOE shape estimation and contact localization modules can be deployed to reconstruct an occluded surface with averaged errors of 3.62 mm. A limitation of this study is that the approximate pose of the subject is known for the purpose of planning the contact locations and trajectories. In the future,



(a) Ground-truth head (front) (b) Ground-truth head (back) (c) Task-dependent prior (front) (d) Task-dependent prior (back)

Fig. 10: **Contacting Surface Reconstruction.** We visualize the contacting surface reconstruction of Head (Wig) object as the watertight red wireframe over (a-b) ground-truth head in blue, and (c-d) task-dependent prior in green.

the system will be extended to autonomously reason about the limb poses and demonstrated with human subjects.

REFERENCES

- [1] Jérémie Allard, Stéphane Cotin, François Faure, Pierre-Jean Bensoussan, François Poyer, Christian Duriez, Hervé Delingette, and Laurent Grisoni. Sofa—an open source framework for medical simulation. In *MMVR 15-Medicine Meets Virtual Reality*, volume 125, pages 13–18. IOP Press, 2007.
- [2] Maria Bauza, Antonia Bronars, and Alberto Rodriguez. Tac2pose: Tactile object pose estimation from the first touch. *The International Journal of Robotics Research*, 42(13):1185–1209, 2023.
- [3] James M Bern, Yannick Schnider, Pol Banzet, Nitish Kumar, and Stelian Coros. Soft robot control with a learned differentiable model. In *2020 3rd IEEE International Conference on Soft Robotics (RoboSoft)*, pages 417–423. IEEE, 2020.
- [4] Aditya Bhatt, Adrian Sieler, Steffen Puhlmann, and Oliver Brock. Surprisingly robust in-hand manipulation: An empirical study. In *Robotics: Science and Systems XVIII*, 2022.
- [5] Tapomayukh Bhattacharjee, Maria E Cabrera, Anat Caspi, Maya Cakmak, and Siddhartha S Srinivasa. A community-centered design framework for robot-assisted feeding systems. In *Proceedings of the 21st International ACM SIGACCESS Conference on Computers and Accessibility*, pages 482–494, 2019.
- [6] Tapomayukh Bhattacharjee, Gilwoo Lee, Hanjun Song, and Siddhartha S Srinivasa. Towards robotic feeding: Role of haptics in fork-based food manipulation. *IEEE Robotics and Automation Letters*, 4(2):1485–1492, 2019.
- [7] Steven W Brose, Douglas J Weber, Ben A Salatin, Garret G Grindle, Hongwu Wang, Juan J Vazquez, and Rory A Cooper. The role of assistive robotics in the lives of persons with disability. *American Journal of Physical Medicine & Rehabilitation*, 89(6):509–521, 2010.
- [8] Daniel Bruder, Xun Fu, R Brent Gillespie, C David Remy, and Ram Vasudevan. Data-driven control of soft robots using koopman operator theory. *IEEE Transactions on Robotics*, 37(3):948–961, 2020.
- [9] Berk Calli, Aaron Walsman, Arjun Singh, Siddhartha Srinivasa, Pieter Abbeel, and Aaron M Dollar. Benchmarking in manipulation research: Using the yale-cmu-berkeley object and model set. *IEEE Robotics & Automation Magazine*, 22(3):36–52, 2015.
- [10] Gerard Canal, Guillem Alenyà, and Carme Torras. A taxonomy of preferences for physically assistive robots. In *2017 26th IEEE International Symposium on Robot and Human Interactive Communication (RO-MAN)*, pages 292–297. IEEE, 2017.
- [11] Gerard Canal, Guillem Alenyà, and Carme Torras. Adapting robot task planning to user preferences: an assistive shoe dressing example. *Autonomous Robots*, 43(6):1343–1356, 2019.
- [12] Gerard Canal, Carme Torras, and Guillem Alenyà. Are preferences useful for better assistance? a physically assistive robotics user study. *ACM Transactions on Human-Robot Interaction (THRI)*, 10(4):1–19, 2021.
- [13] Tiffany L Chen, Matei Ciocarlie, Steve Cousins, Phillip M Grice, Kelsey Hawkins, Kaijen Hsiao, Charles C Kemp, Chih-Hung King, Daniel A Lazewatsky, Adam Leeper, et al. Robots for humanity: A case study in assistive mobile manipulation. *IEEE Robotics & Automation Magazine, Special issue on Assistive Robotics*, 20(1):30–39, 2013.
- [14] Jeremy A Collins, Cody Houff, Patrick Grady, and Charles C Kemp. Visual contact pressure estimation for grippers in the wild. pages 10947–10954, 2023.
- [15] Hang Dai, Nick Pears, William Smith, and Christian Duncan. Statistical modeling of craniofacial shape and texture. *International Journal of Computer Vision*, 128(2):547–571, Nov 2019. ISSN 1573-1405. doi: 10.1007/s11263-019-01260-7. URL <https://doi.org/10.1007/s11263-019-01260-7>.
- [16] Cosimo Della Santina, Robert K Katzschmann, Antonio Bicchi, and Daniela Rus. Dynamic control of soft robots interacting with the environment. In *2018 IEEE International Conference on Soft Robotics (RoboSoft)*, pages 46–53. IEEE, 2018.
- [17] Cosimo Della Santina, Antonio Bicchi, and Daniela Rus. On an improved state parametrization for soft robots with

- piecewise constant curvature and its use in model based control. *IEEE Robotics and Automation Letters*, 5(2):1001–1008, 2020.
- [18] Nathaniel Dennler, Eura Shin, Maja Matarić, and Stefanos Nikolaidis. Design and evaluation of a hair combing system using a general-purpose robotic arm. In *2021 IEEE/RSJ International Conference on Intelligent Robots and Systems (IROS)*, pages 3739–3746. IEEE, 2021.
- [19] Stanimir Dragiev, Marc Toussaint, and Michael Gienger. Gaussian process implicit surfaces for shape estimation and grasping. In *2011 IEEE International Conference on Robotics and Automation*, pages 2845–2850, 2011. doi: 10.1109/ICRA.2011.5980395.
- [20] Stanimir Dragiev, Marc Toussaint, and Michael Gienger. Gaussian process implicit surfaces for shape estimation and grasping. In *2011 IEEE International Conference on Robotics and Automation*, pages 2845–2850. IEEE, 2011.
- [21] Zackory Erickson, Henry M Clever, Greg Turk, C Karen Liu, and Charles C Kemp. Deep haptic model predictive control for robot-assisted dressing. In *2018 IEEE international conference on robotics and automation (ICRA)*, pages 4437–4444. IEEE, 2018.
- [22] Zackory Erickson, Henry M Clever, Vamsee Gangaram, Greg Turk, C Karen Liu, and Charles C Kemp. Multidimensional capacitive sensing for robot-assisted dressing and bathing. In *2019 IEEE 16th International Conference on Rehabilitation Robotics (ICORR)*, pages 224–231. IEEE, 2019.
- [23] Zackory Erickson, Vamsee Gangaram, Ariel Kapusta, C Karen Liu, and Charles C Kemp. Assistive gym: A physics simulation framework for assistive robotics. In *2020 IEEE International Conference on Robotics and Automation (ICRA)*, pages 10169–10176. IEEE, 2020.
- [24] Zackory Erickson, Henry M Clever, Vamsee Gangaram, Eliot Xing, Greg Turk, C Karen Liu, and Charles C Kemp. Characterizing multidimensional capacitive servoing for physical human–robot interaction. *IEEE Transactions on Robotics*, 39(1):357–372, 2022.
- [25] Aimee Goncalves, Naveen Kuppuswamy, Andrew Beaulieu, Avinash Uttamchandani, Katherine M Tsui, and Alex Alspach. Punyo-1: Soft tactile-sensing upper-body robot for large object manipulation and physical human interaction. In *2022 IEEE 5th International Conference on Soft Robotics (RoboSoft)*, pages 844–851. IEEE, 2022.
- [26] Patrick Grady, Jeremy A Collins, Samarth Brahmbhatt, Christopher D Twigg, Chengcheng Tang, James Hays, and Charles C Kemp. Visual pressure estimation and control for soft robotic grippers. In *2022 IEEE/RSJ International Conference on Intelligent Robots and Systems (IROS)*, pages 3628–3635. IEEE, 2022.
- [27] Patrick Grady, Chengcheng Tang, Samarth Brahmbhatt, Christopher D Twigg, Chengde Wan, James Hays, and Charles C Kemp. Pressurevision: Estimating hand pressure from a single rgb image. In *European Conference on Computer Vision*, pages 328–345. Springer, 2022.
- [28] David A Haggerty, Michael J Banks, Ervin Kamenar, Alan B Cao, Patrick C Curtis, Igor Mezić, and Elliot W Hawkes. Control of soft robots with inertial dynamics. *Science Robotics*, 8(81):eadd6864, 2023.
- [29] Kelsey P Hawkins, Phillip M Grice, Tiffany L Chen, Chih-Hung King, and Charles C Kemp. Assistive mobile manipulation for self-care tasks around the head. In *2014 IEEE Symposium on computational intelligence in robotic rehabilitation and assistive technologies (CIR2AT)*, pages 16–25. IEEE, 2014.
- [30] Josie Hughes, Utku Culha, Fabio Giardina, Fabian Guenther, Andre Rosendo, and Fumiya Iida. Soft manipulators and grippers: A review. *Frontiers in Robotics and AI*, 3:69, 2016.
- [31] Josie Hughes, Thomas Plumb-Reyes, Nicholas Charles, L Mahadevan, and Daniela Rus. Detangling hair using feedback-driven robotic brushing. In *2021 IEEE 4th International Conference on Soft Robotics (RoboSoft)*, pages 487–494. IEEE, 2021.
- [32] Wonjun Hwang and Soo-Chul Lim. Inferring interaction force from visual information without using physical force sensors. *Sensors*, 17(11):2455, 2017.
- [33] Aleksandar Jevtić, Andrés Flores Valle, Guillem Alenyà, Greg Chance, Praminda Caleb-Solly, Sanja Dogramadzi, and Carme Torras. Personalized robot assistant for support in dressing. *IEEE transactions on cognitive and developmental systems*, 11(3):363–374, 2018.
- [34] Micah K Johnson and Edward H Adelson. Retrographic sensing for the measurement of surface texture and shape. In *2009 IEEE Conference on Computer Vision and Pattern Recognition*, pages 1070–1077. IEEE, 2009.
- [35] Jonas Jørgensen, Kirsten Borup Bojesen, and Elizabeth Jochum. Is a soft robot more “natural”? exploring the perception of soft robotics in human–robot interaction. *International Journal of Social Robotics*, pages 1–19, 2022.
- [36] Ariel Kapusta, Zackory Erickson, Henry M Clever, Wenhao Yu, C Karen Liu, Greg Turk, and Charles C Kemp. Personalized collaborative plans for robot-assisted dressing via optimization and simulation. *Autonomous Robots*, 43:2183–2207, 2019.
- [37] Ariel S Kapusta, Phillip M Grice, Henry M Clever, Yash Chitalia, Daehyung Park, and Charles C Kemp. A system for bedside assistance that integrates a robotic bed and a mobile manipulator. *PLoS ONE*, 14(10):e0221854, 2019.
- [38] Michael Kazhdan, Matthew Bolitho, and Hugues Hoppe. Poisson Surface Reconstruction. In Alla Sheffer and Konrad Polthier, editors, *Symposium on Geometry Processing*. The Eurographics Association, 2006. ISBN 3-905673-24-X. doi: 10.2312/SGP/SGP06/061-070.
- [39] Chih-Hung King, Tiffany L Chen, Advait Jain, and Charles C Kemp. Towards an assistive robot that autonomously performs bed baths for patient hygiene. In *2010 IEEE/RSJ International Conference on Intelligent Robots and Systems*, pages 319–324. IEEE, 2010.

- [40] Naveen Kuppuswamy, Alex Alspach, Avinash Uttamchandani, Sam Creasey, Takuya Ikeda, and Russ Tedrake. Soft-bubble grippers for robust and perceptive manipulation. In *2020 IEEE/RSJ International Conference on Intelligent Robots and Systems (IROS)*, pages 9917–9924. IEEE, 2020.
- [41] Mike Lambeta, Po-Wei Chou, Stephen Tian, Brian Yang, Benjamin Maloon, Victoria Rose Most, Dave Stroud, Raymond Santos, Ahmad Byagowi, Gregg Kammerer, et al. Digit: A novel design for a low-cost compact high-resolution tactile sensor with application to in-hand manipulation. *IEEE Robotics and Automation Letters*, 5(3):3838–3845, 2020.
- [42] Zohar Levi and Craig Gotsman. Smooth rotation enhanced as-rigid-as-possible mesh animation. *IEEE transactions on visualization and computer graphics*, 21(2):264–277, 2014.
- [43] Shen Li, Nadia Figueroa, Ankit Shah, and Julie Shah. Provably safe and efficient motion planning with uncertain human dynamics. 2021.
- [44] Shen Li, Theodoros Stouraitis, Michael Gienger, Sethu Vijayakumar, and Julie A Shah. Set-based state estimation with probabilistic consistency guarantee under epistemic uncertainty. *IEEE Robotics and Automation Letters*, 7(3):5958–5965, 2022.
- [45] Fukang Liu, Vaidehi Patil, Zackory Erickson, and Zeynep Temel. Characterization of a meso-scale wearable robot for bathing assistance. In *2022 IEEE International Conference on Robotics and Biomimetics (ROBIO)*, pages 2146–2152. IEEE, 2022.
- [46] Yang Liu, Uksang Yoo, Seungbeom Ha, S Farokh Atashzar, and Farshid Alambeigi. Influence of antagonistic tensions on distributed friction forces of multisegment tendon-driven continuum manipulators with irregular geometry. *IEEE/ASME Transactions on Mechatronics*, 27(5):2418–2428, 2021.
- [47] William E. Lorensen and Harvey E. Cline. Marching cubes: A high resolution 3d surface construction algorithm. In *Proceedings of the 14th Annual Conference on Computer Graphics and Interactive Techniques, SIGGRAPH ’87*, page 163–169, New York, NY, USA, 1987. Association for Computing Machinery. ISBN 0897912276. doi: 10.1145/37401.37422. URL <https://doi.org/10.1145/37401.37422>.
- [48] Rishabh Madan, Skyler Valdez, David Kim, Sujie Fang, Luoyan Zhong, Diego Virtue, and Tapomayukh Bhattacharjee. Rabbit: A robot-assisted bed bathing system with multimodal perception and integrated compliance. *arXiv preprint arXiv:2401.15159*, 2024.
- [49] Pragna Mannam, Kenneth Shaw, Dominik Bauer, Jean Oh, Deepak Pathak, and Nancy Pollard. Designing anthropomorphic soft hands through interaction. In *2023 IEEE-RAS 22nd International Conference on Humanoid Robots (Humanoids)*, pages 1–8. IEEE, 2023.
- [50] Amal Nanavati, Vinitha Ranganeni, and Maya Cakmak. Physically assistive robots: A systematic review of mobile and manipulator robots that physically assist people with disabilities. *Annual Review of Control, Robotics, and Autonomous Systems*, 7, 2023.
- [51] Ciarán T O’Neill, Nathan S Phipps, Leonardo Cappello, Sabrina Paganoni, and Conor J Walsh. A soft wearable robot for the shoulder: Design, characterization, and preliminary testing. In *2017 International Conference on Rehabilitation Robotics (ICORR)*, pages 1672–1678. IEEE, 2017.
- [52] World Health Organization et al. *Global report on health equity for persons with disabilities*. World Health Organization, 2022.
- [53] Daehyung Park, You Keun Kim, Zackory M Erickson, and Charles C Kemp. Towards assistive feeding with a general-purpose mobile manipulator. *arXiv preprint arXiv:1605.07996*, 2016.
- [54] Daehyung Park, Yuuna Hoshi, Harshal P Mahajan, Ho Keun Kim, Zackory Erickson, Wendy A Rogers, and Charles C Kemp. Active robot-assisted feeding with a general-purpose mobile manipulator: Design, evaluation, and lessons learned. *Robotics and Autonomous Systems*, 124:103344, 2020.
- [55] Yong-Lae Park, Bor-rong Chen, Néstor O Pérez-Arcibbia, Diana Young, Leia Stirling, Robert J Wood, Eugene C Goldfield, and Radhika Nagpal. Design and control of a bio-inspired soft wearable robotic device for ankle-foot rehabilitation. *Bioinspiration & biomimetics*, 9(1):016007, 2014.
- [56] Panagiotis Polygerinos, Nikolaus Correll, Stephen A Morin, Bobak Mosadegh, Cagdas D Onal, Kirstin Petersen, Matteo Cianchetti, Michael T Tolley, and Robert F Shepherd. Soft robotics: Review of fluid-driven intrinsically soft devices; manufacturing, sensing, control, and applications in human-robot interaction. *Advanced Engineering Materials*, 19(12):1700016, 2017.
- [57] Tommaso Proietti, Ciaran O’Neill, Lucas Gerez, Tazzy Cole, Sarah Mendelowitz, Kristin Nuckols, Cameron Hohimer, David Lin, Sabrina Paganoni, and Conor Walsh. Restoring arm function with a soft robotic wearable for individuals with amyotrophic lateral sclerosis. *Science Translational Medicine*, 15(681):eadd1504, 2023.
- [58] Kavya Puthuveetil, Charles C Kemp, and Zackory Erickson. Bodies uncovered: Learning to manipulate real blankets around people via physics simulations. *IEEE Robotics and Automation Letters*, 7(2):1984–1991, 2022.
- [59] Kavya Puthuveetil, Sasha Wald, Atharva Pusalkar, Pratyusha Karnati, and Zackory Erickson. Robust body exposure (robe): A graph-based dynamics modeling approach to manipulating blankets over people. *IEEE Robotics and Automation Letters*, 8(10):6299–6306, 2023.
- [60] Yu She, Sandra Q Liu, Peiyu Yu, and Edward Adelson. Exoskeleton-covered soft finger with vision-based proprioception and tactile sensing. In *2020 IEEE International Conference on Robotics and Automation (ICRA)*, pages 10075–10081. IEEE, 2020.

- [61] Adrian Sieler and Oliver Brock. Dexterous soft hands linearize feedback-control for in-hand manipulation. In *2023 IEEE/RSJ International Conference on Intelligent Robots and Systems (IROS)*, pages 8757–8764. IEEE, 2023.
- [62] Nina R Sinatra, Clark B Teeple, Daniel M Vogt, Kevin Kit Parker, David F Gruber, and Robert J Wood. Ultragentle manipulation of delicate structures using a soft robotic gripper. *Science Robotics*, 4(33):eaax5425, 2019.
- [63] Andrea Sipos and Nima Fazeli. Simultaneous contact location and object pose estimation using proprioception and tactile feedback. In *2022 IEEE/RSJ International Conference on Intelligent Robots and Systems (IROS)*, pages 3233–3240. IEEE, 2022.
- [64] Cory-Ann Smarr, Akanksha Prakash, Jenay M Beer, Tracy L Mitzner, Charles C Kemp, and Wendy A Rogers. Older adults’ preferences for and acceptance of robot assistance for everyday living tasks. In *Proceedings of the human factors and ergonomics society annual meeting*, volume 56, pages 153–157. Sage Publications Sage CA: Los Angeles, CA, 2012.
- [65] Olga Sorkine and Marc Alexa. As-rigid-as-possible surface modeling. In *Symposium on Geometry processing*, volume 4, pages 109–116. Citeseer, 2007.
- [66] Zhanyi Sun, Yufei Wang, David Held, and Zackory Erickson. Force-constrained visual policy: Safe robot-assisted dressing via multi-modal sensing. *arXiv preprint arXiv:2311.04390*, 2023.
- [67] Priya Sundaresan, Suneel Belkhale, and Dorsa Sadigh. Learning visuo-haptic skewering strategies for robot-assisted feeding. In *Conference on Robot Learning*, pages 332–341. PMLR, 2023.
- [68] Sudharshan Suresh, Zilin Si, Joshua G Mangelson, Wenzhen Yuan, and Michael Kaess. Shapemap 3-d: Efficient shape mapping through dense touch and vision. In *2022 International Conference on Robotics and Automation (ICRA)*, pages 7073–7080. IEEE, 2022.
- [69] Sudharshan Suresh, Haozhi Qi, Tingfan Wu, Taosha Fan, Luis Pineda, Mike Lambeta, Jitendra Malik, Mriinal Kalakrishnan, Roberto Calandra, Michael Kaess, et al. Neural feels with neural fields: Visuo-tactile perception for in-hand manipulation. *arXiv preprint arXiv:2312.13469*, 2023.
- [70] Javier Tapia, Espen Knoop, Mojmir Mutný, Miguel A Otaduy, and Moritz Bächer. Makesense: Automated sensor design for proprioceptive soft robots. *Soft robotics*, 7(3):332–345, 2020.
- [71] Tze Ho Elden Tse, Zhongqun Zhang, Kwang In Kim, Ales Leonardis, Feng Zheng, and Hyung Jin Chang. S 2 contact: Graph-based network for 3d hand-object contact estimation with semi-supervised learning. In *European Conference on Computer Vision*, pages 568–584. Springer, 2022.
- [72] Mark J. Van der Merwe, Youngsun Wi, Dmitry Berenson, and Nima Fazeli. Integrated object deformation and contact patch estimation from visuo-tactile feedback. In *Robotics: Science and Systems XIX*, 2023.
- [73] Maria Bauza Villalonga, Alberto Rodriguez, Bryan Lim, Eric Valls, and Theo Sechopoulos. Tactile object pose estimation from the first touch with geometric contact rendering. In *Conference on Robot Learning*, pages 1015–1029. PMLR, 2021.
- [74] Hongbo Wang, Massimo Totaro, and Lucia Beccai. Toward perceptive soft robots: Progress and challenges. *Advanced Science*, 5(9):1800541, 2018.
- [75] Ruoyu Wang, Shiheng Wang, Songyu Du, Erdong Xiao, Wenzhen Yuan, and Chen Feng. Real-time soft body 3d proprioception via deep vision-based sensing. *IEEE Robotics and Automation Letters*, 5(2):3382–3389, 2020.
- [76] Yue Wang, Yongbin Sun, Ziwei Liu, Sanjay E Sarma, Michael M Bronstein, and Justin M Solomon. Dynamic graph cnn for learning on point clouds. *ACM Transactions on Graphics (tog)*, 38(5):1–12, 2019.
- [77] Yufei Wang, Zhanyi Sun, Zackory Erickson, and David Held. One policy to dress them all: Learning to dress people with diverse poses and garments. In *Robotics: Science and Systems XIX*, 2023.
- [78] Benjamin Ward-Cherrier, Nicholas Pestell, Luke Cramphorn, Benjamin Winstone, Maria Elena Giannaccini, Jonathan Rossiter, and Nathan F Lepora. The tactip family: Soft optical tactile sensors with 3d-printed biomimetic morphologies. *Soft robotics*, 5(2):216–227, 2018.
- [79] Youngsun Wi, Pete Florence, Andy Zeng, and Nima Fazeli. Virdo: Visio-tactile implicit representations of deformable objects. In *2022 International Conference on Robotics and Automation (ICRA)*, pages 3583–3590. IEEE, 2022.
- [80] Youngsun Wi, Andy Zeng, Pete Florence, and Nima Fazeli. Virdo++: Real-world, visuo-tactile dynamics and perception of deformable objects. In *6th Annual Conference on Robot Learning*, 2022.
- [81] Rebecca Wiczorek, Megan A Bayles, and Wendy A Rogers. Domestic robots for older adults: Design approaches and recommendations. *Design of Assistive Technology for Ageing Populations*, pages 203–219, 2020.
- [82] Joshua M Wiener, Raymond J Hanley, Robert Clark, and Joan F Van Nostrand. Measuring the activities of daily living: Comparisons across national surveys. *Journal of gerontology*, 45(6):S229–S237, 1990.
- [83] Oliver Williams and Andrew Fitzgibbon. Gaussian process implicit surfaces. In *Gaussian Processes in Practice*, 2006.
- [84] Akihiko Yamaguchi and Christopher G Atkeson. Combining finger vision and optical tactile sensing: Reducing and handling errors while cutting vegetables. In *2016 IEEE-RAS 16th International Conference on Humanoid Robots (Humanoids)*, pages 1045–1051. IEEE, 2016.
- [85] Uksang Yoo, Yang Liu, Ashish D Deshpande, and Farshid Alamabeigi. Analytical design of a pneumatic

- elastomer robot with deterministically adjusted stiffness. *IEEE robotics and automation letters*, 6(4):7773–7780, 2021.
- [86] Uksang Yoo, Hanwen Zhao, Alvaro Altamirano, Wenzhen Yuan, and Chen Feng. Toward zero-shot sim-to-real transfer learning for pneumatic soft robot 3d proprioceptive sensing. In *2023 IEEE International Conference on Robotics and Automation (ICRA)*, pages 544–551. IEEE, 2023.
 - [87] Uksang Yoo, Ziven Lopez, Jeffrey Ichnowski, and Jean Oh. Poe: Acoustic soft robotic proprioception for omnidirectional end-effectors, 2024.
 - [88] Leanne Young, Gregory T Rule, Robert T Bocchieri, Timothy J Walilko, Jennie M Burns, and Geoffrey Ling. When physics meets biology: low and high-velocity penetration, blunt impact, and blast injuries to the brain. *Frontiers in neurology*, 6:89, 2015.
 - [89] Wenzhen Yuan, Siyuan Dong, and Edward H Adelson. Gelsight: High-resolution robot tactile sensors for estimating geometry and force. *Sensors*, 17(12):2762, 2017.
 - [90] Fan Zhang and Yiannis Demiris. Learning garment manipulation policies toward robot-assisted dressing. *Science Robotics*, 7(65):eabm6010, 2022.
 - [91] Athanasia Zlatintsi, AC Dometios, Nikolaos Kardaris, Isidoros Rodomagoulakis, Petros Koutras, X Papageorgiou, Petros Maragos, Costas S Tzafestas, Panagiotis Vartholomeos, Klaus Hauer, et al. I-support: A robotic platform of an assistive bathing robot for the elderly population. *Robotics and Autonomous Systems*, 126: 103451, 2020.
 - [92] Gabriel Zöller, Vincent Wall, and Oliver Brock. Active acoustic contact sensing for soft pneumatic actuators. In *2020 IEEE International Conference on Robotics and Automation (ICRA)*, pages 7966–7972. IEEE, 2020.